ChemPubSoc Europe

DOI: 10.1002/cssc.201402469

Silicon Nanowire Photocathodes for Light-Driven Electroenzymatic Synthesis

Sahng Ha Lee, Gyeong Min Ryu, Dong Heon Nam, Jae Hong Kim, and Chan Beum Park*[a]

The photoelectroenzymatic synthesis of chemical compounds employing platinum nanoparticle-decorated silicon nanowires (Pt-SiNWs) is presented. The Pt-SiNWs proved to be an efficient material for photoelectrochemical cofactor regeneration because the silicon nanowires absorbs a wide range of the solar spectrum while the platinum nanoparticle serve as an excellent catalyst for electron and proton transfer. By integrating the platform with redox enzymatic reaction, visible-light-driven electroenzymatic synthesis of L-glutamate was achieved. Compared to electrochemical and photochemical methods, this approach is free from side reactions caused by sacrificial electron donors and has the advantage of applying low potential to realize energy-efficient and sustainable synthesis of chemicals by a photoelectroenzymatic system.

Numerous oxidoreductases critically require pyridine nucleotide cofactors [NAD(P)H] as a redox counterpart to maintain their catalytic turnover.[1] Over the past decades, many efforts have been made to regenerate NAD(P)H in situ through enzymatic or nonenzymatic routes. According to a recent Review by Hollmann et al.,[2] electrochemical regeneration of NAD(P)H offers advantages of low costs, no co-substrate requirement, and mass-free electron delivery from an electrode compared to enzymatic regeneration. However, direct NAD(P)H regeneration requires two-step reduction at high potential, approximately −1.1 V and −1.7 V vs. SCE, yielding enzymatically inactive NAD dimers and isomers. The side-effect can be prevented by the use of a redox mediator such as a rhodium-based organometallic complex (**M**; $([Cp^*Rh(bpy)H_2O]^{2+}$, $Cp^* = C_5Me_5$, bpy = 2,2′-bipyridine) that enables efficient and simultaneous two-electron transfer from an electrode to NAD^+. On the other hand, visible light-driven, photochemical regeneration of NAD(P)H had recently been attempted using organic and inorganic photosensitizers (e.g., xanthenes, porphyrins, quantum dots, and metal oxides).[3] One of the challenging issues in photochemical regeneration is the requirement of sacrificial agents, such as triethanolamine (TEOA), as electron donors to empty the highest occupied molecular orbital level (HOMO or valence band) of photosensitizers.[4] The accumulation of oxidized byproducts (e.g., glycoaldehyde and diethanolamine from TEOA oxidation)[5] should be avoided for the development of sustainable photoenzymatic processes. Furthermore, high concentration of sacrificial agents can lead to undesirable side reactions that inhibit cofactor regeneration and redox enzymatic reactions.

Herein, we report on photoelectrochemical cofactor regeneration that can address the disadvantages of both the photo- and electrochemical approaches by not requiring sacrificial electron donors and high applied potentials. We develop silicon nanowire (SiNW) arrays as a photocathode for visible-light-driven electrochemical reduction of the rhodium-based organometallic mediator, **M**, to regenerate enzymatically active NADH from NAD^+. Silicon is an attractive light-harvesting material because it is robust, abundant, and efficient for solar energy conversion.[6] Furthermore, its bandgap is well suited to absorb a wide range of the solar spectrum.[7] Due to the quantum confinement effect, SiNWs possess adjustable bandgaps (e.g., 1.1 eV)[8] through control of nanowire morphology, which enables photocatalytic conversions to occur under visible light unlike planar silicon or other wide-bandgap semiconducting materials such as TiO_2 and ZnO ($E_g \approx 3.2$ eV).[7b,9]

As depicted in Figure 1, we connected the SiNW photocathode to an external bias, providing enough power for electrons to overcome the activation energy and to transfer excited electrons to the mediator, reducing $\mathbf{M_{ox}}$ $\{[Cp^*Rh(bpy)H_2O]^{2+}\}$ to $\mathbf{M_{red1}}$ $\{[Cp^*Rh(bpy)]\}$. Then, $\mathbf{M_{red1}}$ was further reduced to $\mathbf{M_{red2}}$ $\{[Cp^*Rh(bpy)H]^+\}$ by taking one proton up from the buffer solution, and hydride ion was transferred from $\mathbf{M_{red2}}$ to NAD^+ to regenerate NADH, returning $\mathbf{M_{red2}}$ to the initial state

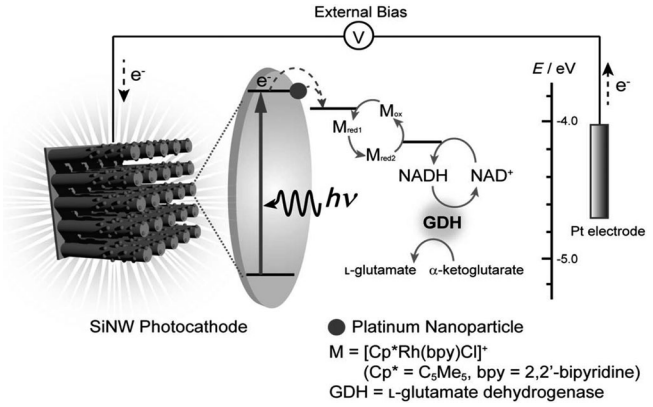

Figure 1. Schematic illustration of the photo-electroenzymatic reaction using a silicon nanowire (SiNW) photocathode. Photons absorbed by SiNWs generate excited electrons, which drift to the electrode/solution interface and reduce **M**. A chain of NADH regeneration occurs in the sequence of photo-induced electron transfer. Finally, the regenerated NADH is used to convert α-ketoglutarate to L-glutamate using GDH.

[a] *Dr. S. H. Lee,[+] G. M. Ryu,[+] D. H. Nam, Dr. J. H. Kim, Prof. C. B. Park*
Department of Materials Science and Engineering
Korea Advanced Institute of Science and Technology (KAIST)
335 Science Road, Yuseong-gu, Daejeon 305-701 (South Korea)
E-mail: parkcb@kaist.ac.kr

[+] *These authors contributed equally to this work.*

Supporting Information for this article is available on the WWW under http://dx.doi.org/10.1002/cssc.201402469.

$\mathbf{M_{ox}}$. Finally, photoelectrochemically regenerated NADH was used as a redox equivalent for enzymatic synthesis, that is, the conversion of α-ketoglutarate to L-glutamate by glutamate dehydrogenase (GDH). The holes generated at the valence band of SiNWs were compensated for by electrons supplied from an external power source, not with a sacrificial agent.

We synthesized vertically aligned SiNWs through the metal-catalyzed electroless etching (MCEE) process,[10] as illustrated in Figure S1 A in the Supporting Information. According to scanning electron microscopy (SEM) images (Supporting Information, Figure S2 A), the average length of SiNWs was approximately 20 μm and their diameter was in the range of 100–200 nm after 30 min of etching. We terminated thus-prepared SiNWs with hydrogen by immersing them in an HF solution to suppress electron–hole pair recombination and promote efficient electron transfer from an electrode to the electron mediator.[11] We observed that the photocurrent generated by bare SiNW photocathodes before the hydrogen termination was almost negligible compared to that of the hydrogen-terminated ones that exhibited strong photoresponses (Figure 2a; Supporting Information, Figure S3). According to the cyclic voltammogram of the hydrogen-terminated SiNW electrode (Supporting Information, Figure S4), there was a strong reduction current at over −0.6 V under illumination by visible light while a negligible current was observed under dark conditions.

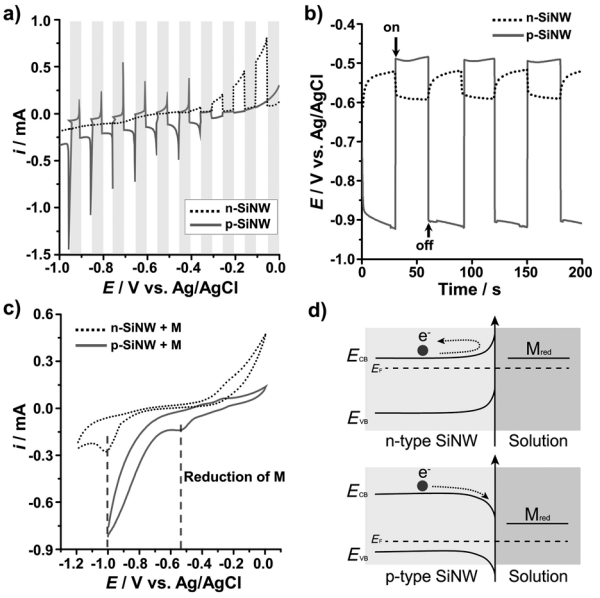

Figure 2. a) The photocurrent of n-type and p-type hydrogen-terminated silicon nanowires (n-SiNW and p-SiNW) with a linear sweep voltammetry mode under alternating conditions of darkness and light. b) The chronopotentiometry curves of n-type and p-type SiNWs under a cathodic current of −10 μA show light-driven voltage changes in the opposite direction. c) Cyclic voltammograms of n-SiNW and p-SiNW in the presence of **M** (250 μM). The reduction of **M** occurs at −0.54 V and −1.0 V for p-SiNW and n-SiNW, respectively. d) A schematic diagram of electronic energy levels at the interface between n-type and p-type SiNWs and a solution containing **M**. The energy band bends upwards and creates a barrier in the n-SiNW while the downward band-bending is induced in p-SiNW.

The electronic band structure at the interface between a semiconducting electrode and an electrolyte varies depending on the type of the semiconductor.[12] To compare the effect of band bending on photocathode performance, we fabricated p-type and n-type silicon nanowire (p-SiNW and n-SiNW) electrodes, respectively, and analyzed their photoelectrochemical characteristics using linear sweep voltammetry and chronopotentiometry (Figure 2a, b). The two different types of photocathodes exhibited opposite signals of photocurrent and photoinduced potential change under constant cathodic current (−10 μA). In the case of the p-SiNW photocathode, we observed an increase in the cathodic current along with a positive shift of photoinduced potential by 0.4 V, while the n-SiNW photocathode showed an anodic photocurrent increase and a negative potential shift of 0.06 V. This result indicates that the power required for current generation under illumination decreases with p-SiNWs but increases with n-SiNWs. We further investigated the reduction of **M** on differently doped SiNW electrodes (Figure 2c). According to the literature,[13] $\mathbf{M_{ox}}$ accepts two electrons from the electrode at a potential of around −0.75 V, followed by an irreversible chemical transformation to $\mathbf{M_{red2}}$ via proton uptake. Interestingly, we observed different degrees of shift in the reduction potential of **M** depending on the doping type of SiNWs.

While there was no reduction of **M** under dark conditions in both cases (data not shown), the reduction peak of **M** appeared at around −0.54 V (for p-SiNWs) and −1.0 V (for n-SiNWs) upon illumination, which can be interpreted as cathodic and anodic shifts of reduction peaks, respectively. The result is attributed to the equilibrium change of SiNWs' Fermi level (E_F) by different dopants (Figure 2d).[14] In the case of p-SiNWs, boron is doped to create an additional positive charge carrier; thus, the E_F of p-SiNWs is positioned closer to the valence band, which results in the band bending towards anodic potential at the electrode-solution interface. In the case of n-SiNWs, in contrast, the dopant (phosphorous) provides an additional electron to make the E_F of n-SiNWs greater than that of the intrinsic semiconductor and position it closer to the conduction band. Hence, band-bending occurs upwards to create an energy barrier in n-SiNWs, requiring a higher externally applied bias than in p-SiNWs.[15] Taken together, the p-SiNW photocathode is suitable for photoelectrochemical NADH regeneration since the p-SiNW electrode exhibits cathodic potential shift in the reduction of **M** and a lower energy barrier for the transfer of electrons to **M**.

We investigated the electrocatalytic effect of the p-SiNW photocathode on NADH regeneration. As shown in Figure 3a, we observed an increase in cathodic peak current and a potential shift in the presence of **M** and NAD^+ due to the electrocatalytic reduction of NAD^+ by **M**. The efficient photoexcited electron transfer from p-SiNWs to **M** was proved by significantly enhanced photocurrent generation on p-SiNWs (Figure 3b). It improved the catalytic turnover rate of **M**, increasing the rate of NADH regeneration below the reduction potential of **M**. At the applied potential of −0.8 V, the rate of photoelectrochemical NADH regeneration increased approximately six times under light illumination compared to that under dark. At

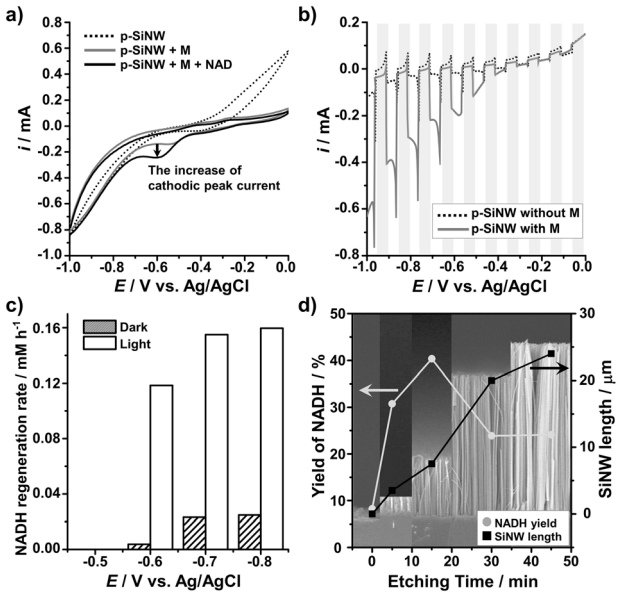

Figure 3. a) Cyclic voltammogram curves show the increase of the cathodic peak current indicating the catalytic effect of **M** (250 μM) on reducing NAD^+ (1 mM) to NADH. b) Linear sweep voltammogram of p-SiNW in the presence and absence of **M** (250 μM). The light was switched on and off every 5 s. c) Photoelectrochemical reduction of NADH under various applied potentials with and without light. The initial NAD^+ concentration was 1 mM. d) Photoelectrochemical NADH regeneration performance under external bias of −0.8 V and the length of silicon nanowires with etching times of 5, 15, 30, and 45 min. The SEM images of SiNW for each etching time are in the background.

the applied voltage of −0.6 V, which is much lower than the reduction potential of **M** (−0.75 V), the photocathodic effect of p-SiNWs was observed clearly. While electrochemical regeneration of NADH—under dark conditions—did not occur, approximately 0.18 mM of NADH was regenerated in 90 min with light irradiation. When more than −0.8 V was applied, a comparable amount of NADH was regenerated even under dark conditions through electrochemical route. Since nanowire length can affect carrier-collection efficiency,[7a] we further studied the effects of SiNW length on the performance of photoelectrochemical NADH regeneration. For this experiment, we controlled the length of SiNWs by changing etching time (5, 15, 30, and 45 min) during the lithographic fabrication process (Figure S1 a) and observed a proportional relationship between etching time and nanowire length. The yield of NADH regeneration showed a volcano-plot-like behavior and exhibited the maximum catalytic performance with 15 min of etching (Figure 3 d). According to the literature,[16] an optimum point exists in the relationship between photocatalyst concentration and catalytic reaction rate. A high density of the array of SiNWs reduces the penetration depth and increases the scattering of the incident light,[16] which should lead to the decrease of NADH regeneration yield with longer SiNWs than 10 μm.

Hybridized with metal nanoparticles (e.g., Pt, Au, Ag), SiNWs enhance the photocatalytic activity for H^+/H_2 redox reactions due to fast charge separation and plasmon resonance energy transfer.[17] Platinum nanoparticles (PtNPs), especially, serve to donate protons and electrons to **M** for efficient electrochemical and photochemical NADH regeneration.[18] In the current work, we have incorporated PtNPs into the bare p-SiNW photocathode for the improvement of photoelectrochemical NADH regeneration efficiency. Pt-decorated silicon nanowires (Pt-SiNWs) were synthesized by electroless metal deposition (EMD)[9b] through the immersion of SiNW electrode in a H_2PtCl_6 solution for 10 min. We analyzed the formation of Pt-SiNWs using scanning and transmission electron microscopy. As shown in Figure 4 a and Figure S2 B, PtNPs with approximately

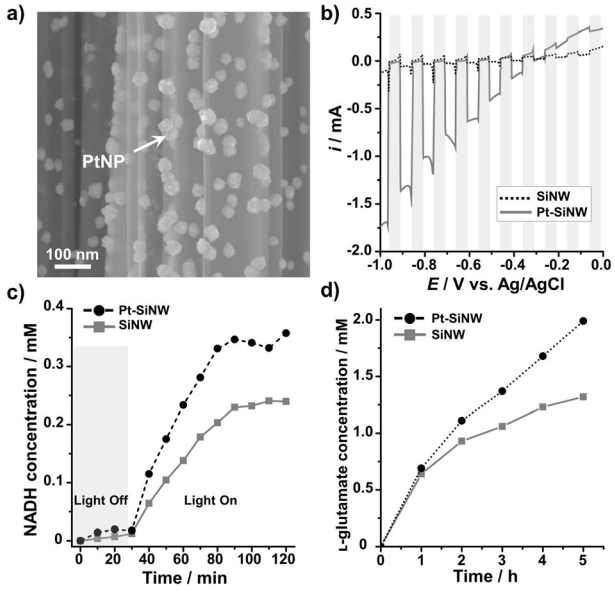

Figure 4. a) SEM image of platinum nanoparticles (PtNPs) decorated on the surface of SiNWs. b) Photocurrent responses of the bare p-type SiNW (marked as SiNW) and Pt-SiNW photocathodes versus ON–OFF cycles of illumination. c) Photoelectrochemical NADH regeneration, and d) photo-electroenzymatic conversion of α-ketoglutarate into L-glutamate of bare SiNW and Pt-SiNW were conducted under visible light ($\lambda > 420$ nm) at −0.8 V of applied bias. Light was switched on after 30 min of the dark reaction in NADH regeneration.

30 nm diameter were synthesized and distributed along the SiNWs. Energy-dispersive X-ray spectroscopic analysis confirmed that the nanoparticles on the surface of SiNWs are made of platinum. We further studied the photoelectrochemical properties of Pt-SiNWs using linear sweep and cyclic voltammetry. Under visible-light irradiation ($\lambda > 420$ nm), the photocurrent intensity (−1 mA) at −0.8 V (vs. Ag/AgCl) of Pt-SiNWs was approximately 30 times higher than that (−0.03 mA) of bare SiNWs (Figure 4 b), indicating that the PtNPs boosted the charge separation of SiNWs as an electron acceptor. In addition, we observed a strong cathodic current at −0.4 V (vs. Ag/AgCl) of Pt-SiNWs under visible light (Supporting Information, Figure S5), suggesting that PtNPs contribute to efficient electron and proton transfer by reducing reaction impedance in agreement with the literature.[19] Protons adsorbed on noble metal particles, such as platinum and palladium, form an intermediate state (noble metal–H_{ads}) and can function as a reducing agent for organic molecules.[20] In this study Pt–H_{ads} on the surface of SiNW should accelerate NADH regeneration by two

routes, donating a proton to $\mathbf{M}_{red1}$ and shuttling electrons from SiNWs to $\mathbf{M}_{ox}$.

To confirm the role of PtNPs on SiNWs, we tested visible light-driven NADH regeneration by Pt-SiNWs with the applied voltage of −0.8 V. As shown in Figure 4c, the catalytic activity of PtNPs significantly enhanced both turnover number and turnover frequency of **M** from 0.96 and 0.035 s^{-1} to 1.44 and 0.065 s^{-1}, respectively. To achieve biocatalytic artificial photosynthesis, we coupled photoelectrochemical NADH regeneration with a redox enzymatic reaction using L-glutamate dehydrogenase (GDH) as a model enzyme that can produce L-glutamate from α-ketoglutarate in the presence of enzymatically active NADH. Under −0.8 V (vs. Ag/AgCl) of applied potential after 5 h of illumination, the concentration of synthesized L-glutamate with Pt-SiNWs was measured as 1.54-fold higher than that with bare SiNWs (Figure 4d). The persistent photoelectroenzymatic reaction with Pt-SiNW in comparison to SiNW further indicates enhanced stability of SiNW photocathode by the incorporation of PtNPs, as reported previously.[6]

In summary, we successfully demonstrate visible light-enhanced electroenzymatic synthesis using silicon nanowire (SiNW) photocathodes. The photoelectrochemical approach does not need any sacrificial electron donor, though such is donor is a critical requirement for traditional photochemical cofactor regeneration. Furthermore, visible-light absorption by SiNWs allows to lower the applied potential more than in the case of electrochemical NADH regeneration. Based on multiple electrochemical analyses of different types of SiNWs, we reveal that p-type SiNWs can transfer photoexcited electrons efficiently to NAD^+ through **M**, an electron mediator. Under visible-light illumination, the NADH regeneration rate is six times higher than that under dark conditions, which is partly due to the photocatalytic effect of SiNWs. While an optimum length of SiNWs exists for their best performance, platinum nanoparticles (PtNPs) deposited at the surface of SiNWs as an electrocatalyst significantly enhance the rate of NADH regeneration and the yield of redox enzymatic synthesis. Our work shows that Pt–SiNWs is a promising photocathode material for redox enzymatic reactions coupled with photoelectrochemical NADH regeneration to synthesize valuable chemicals by diverse cofactor-dependent biocatalysts without sacrificial electron donor and high overpotential.

Experimental Section

Materials: Unless noted otherwise, all chemicals including hydrofluoric acid (HF), silver nitrate ($AgNO_3$), hydrogen peroxide (H_2O_2), nitric acid (HNO_3), chloroplatinic acid hexahydrate ($H_2PtCl_6{\cdot}6H_2O$), β-nicotinamide adenine dinucleotide hydrate (NAD^+), ammonium sulfate [$(NH_4)_2SO_4$], L-glutamic dehydrogenase from bovine liver (GDH), and α-ketoglutaric acid disodium salt dehydrate were purchased from Sigma–Aldrich (USA). Lightly doped (1–10 Ω cm for p-type, 1–30 Ω cm for n-type) silicon wafers (100) were obtained from Tasco (Korea). The rhodium complex {$[Cp^*Rh(bpy)(H_2O)]^{2+}$}, **M**, was synthesized according to a literature report.[18b]

Silicon nanowire electrode preparation: Silicon nanowires (SiNWs) were synthesized by the metal-assisted chemical etching method according to a literature report.[10] Briefly, a silicon wafer was cut to a size of 10 mm × 40 mm and cleaned with acetone, ethanol, 2-propanol, and piranha solutions for 10 min each. The cleaned silicon wafer was rinsed with deionized water several times and immersed in a 5% HF solution for 3 min. Then, the wafer was placed into a solution of $AgNO_3$ (5 mM) and HF (4.8 M) for 1 min to deposit silver nanoparticles onto the wafer. Silver nanoparticles etched down the Si wafer vertically in a solution of H_2O_2 (0.4 M) and HF (4.8 M). To control the length of SiNWs, we varied the etching time from 5 to 45 min. After sufficient etching, the silver nanoparticles were removed by bathing the Si wafer in a diluted nitric acid solution. The as-synthesized silicon nanowires were immersed in a 5% HF solution for hydrogen termination and decorated with platinum nanoparticles through the immersion of SiNWs into H_2PtCl_6 (1 mM) and HF (4.8 M) solution for 10 min. In order to create the working electrode, SiNWs were cut into 10 × 10 mm sections and connected to a copper wire using carbon paste. Next, SiNWs and carbon paste were covered with insulating epoxy resin with the exception of the specific area to be exposed.

Characterization: The morphology of silicon nanowires was analyzed using an S-4800 field emission scanning electron microscope (Hitachi High-Technologies Co., Japan) and 300 keV field-emission transmission electron microscope (FEI, Model Tecnai G^2 F30 S-Twin, Netherlands). UV/Vis absorption spectra were measured using a V-650 spectrophotometer (JASCO Inc., Japan). The photocurrent was measured in a three-electrode configuration using Ag/AgCl in 3 M NaCl (0.197 V vs. standard hydrogen electrode) as a reference electrode, a platinum wire as a counter electrode, and an SiNW electrode as a working electrode in a solution of phosphate buffer (50 mM, pH 7.5). The system was connected to a potentiostat/galvanostat (WonATech, Model WMPG1000, Korea) under a 450 W Xe lamp illumination with a 420 nm cut-off filter. Cyclic voltammetry was scanned at a rate of 50 mV s^{-1} and linear sweep voltammetry was scanned at a rate of 10 mV s^{-1}.

NADH regeneration and enzymatic synthesis of L-glutamate: Photoelectrochemical NADH regeneration of SiNW photocathode was conducted in a three-electrode system under a 450 W Xe lamp illumination with a 420 nm cut-off filter for visible-light excitation of photons. SiNW electrodes were immersed in a phosphate buffer solution (50 mM, pH 7.5) containing 1 mM NAD^+ and 250 μM **M**. During NADH regeneration, the concentrations of NAD^+ and NADH were measured from peak intensities of absorption at 260 nm and 340 nm, respectively. The enzyme reaction with 40 U of GDH was carried out in a phosphate buffer (50 mM, pH 7.5) with 1 mM NAD^+, 250 μM **M**, 5 mM α-ketoglutarate, and 0.1 M $(NH_4)_2SO_4$.

Acknowledgements

This study was supported by grants from the National Research Foundation (NRF) via the National Leading Research Laboratory (NRF-2013R1A2A1A05005468) and the Intelligent Synthetic Biology Center of Global Frontier R&D Project (2011–0031957), Republic of Korea.

Keywords: artificial photosynthesis · biocatalysis · cofactors · photochemistry · silicon

[1] W. A. van der Donk, H. Zhao, *Curr. Opin. Biotechnol.* **2003**, *14*, 421–426.
[2] F. Hollmann, I. W. C. E. Arends, K. Buehler, *ChemCatChem* **2010**, *2*, 762–782.
[3] a) S. H. Lee, D. H. Nam, C. B. Park, *Adv. Synth. Catal.* **2009**, *351*, 2589–2594; b) J. S. Lee, D. H. Nam, S. K. Kuk, C. B. Park, *Chem. Eur. J.* **2014**, *20*, 3584–3588; c) M. Lee, J. U. Kim, J. S. Lee, B. I. Lee, J. Shin, C. B. Park,

Adv. Mater. **2014**, *26*, 4463 – 4468; d) S. H. Lee, D. H. Nam, J. H. Kim, J.-O. Baeg, C. B. Park, *ChemBioChem* **2009**, *10*, 1621 – 1624; e) J. Ryu, S. H. Lee, D. H. Nam, C. B. Park, *Adv. Mater.* **2011**, *23*, 1883 – 1888.
[4] a) S. H. Lee, J. H. Kim, C. B. Park, *Chem. Eur. J.* **2013**, *19*, 4392 – 4406; b) J. H. Kim, D. H. Nam, C. B. Park, *Curr. Opin. Biotechnol.* **2014**, *28*, 1 – 9.
[5] X.-J. Yang, B. Chen, L.-Q. Zheng, L.-Z. Wu, C.-H. Tung, *Green Chem.* **2014**, *16*, 1082 – 1086.
[6] X. Wang, K.-Q. Peng, X.-J. Pan, X. Chen, Y. Yang, L. Li, X.-M. Meng, W.-J. Zhang, S.-T. Lee, *Angew. Chem. Int. Ed.* **2011**, *50*, 9861 – 9865; *Angew. Chem.* **2011**, *123*, 10035 – 10039.
[7] a) K.-Q. Peng, S.-T. Lee, *Adv. Mater.* **2011**, *23*, 198 – 215; b) Y. Qu, X. Zhong, Y. Li, L. Liao, Y. Huang, X. Duan, *J. Mater. Chem.* **2010**, *20*, 3590 – 3594.
[8] a) M. Nolan, S. O'Callaghan, G. Fagas, J. C. Greer, T. Frauenheim, *Nano Lett.* **2007**, *7*, 34 – 38; b) X. Zhao, C. M. Wei, L. Yang, M. Y. Chou, *Phys. Rev. Lett.* **2004**, *92*, 236805.
[9] a) I. Oh, J. Kye, S. Hwang, *Nano Lett.* **2011**, *12*, 298 – 302; b) K.-Q. Peng, X. Wang, X.-L. Wu, S.-T. Lee, *Nano Lett.* **2009**, *9*, 3704 – 3709.
[10] M.-L. Zhang, K.-Q. Peng, X. Fan, J.-S. Jie, R.-Q. Zhang, S.-T. Lee, N.-B. Wong, *J. Phys. Chem. C* **2008**, 112, 4444 – 4450.
[11] M. Shao, L. Cheng, X. Zhang, D. D. D. Ma, S.-t. Lee, *J. Am. Chem. Soc.* **2009**, *131*, 17738 – 17739.
[12] C. A. Koval, J. N. Howard, *Chem. Rev.* **1992**, *92*, 411 – 433.
[13] F. Hollmann, A. Schmid, E. Steckhan, *Angew. Chem. Int. Ed.* **2001**, *40*, 169 – 171; *Angew. Chem.* **2001**, *113*, 190 – 193.
[14] N. S. Lewis, *Inorg. Chem.* **2005**, *44*, 6900 – 6911.
[15] M. Grätzel, *Nature* **2001**, *414*, 338 – 344.
[16] H. Kisch, *Angew. Chem. Int. Ed.* **2013**, *52*, 812 – 847; *Angew. Chem.* **2013**, *125*, 842 – 879.
[17] a) A. Tanaka, K. Hashimoto, H. Kominami, *J. Am. Chem. Soc.* **2014**, *136*, 586 – 589; b) S. Mubeen, J. Lee, N. Singh, S. Kramer, G. D. Stucky, M. Moskovits, *Nat. Nanotechnol.* **2013**, *8*, 247 – 251.
[18] a) J. H. Kim, M. Lee, J. S. Lee, C. B. Park, *Angew. Chem. Int. Ed.* **2012**, *51*, 517 – 520; *Angew. Chem.* **2012**, *124*, 532 – 535; b) H.-K. Song, S. H. Lee, K. Won, J. H. Park, J. K. Kim, H. Lee, S.-J. Moon, D. K. Kim, C. B. Park, *Angew. Chem. Int. Ed.* **2008**, *47*, 1749 – 1752; *Angew. Chem.* **2008**, *120*, 1773 – 1776.
[19] A. Heller, E. Aharon-Shalom, W. A. Bonner, B. Miller, *J. Am. Chem. Soc.* **1982**, *104*, 6942 – 6948.
[20] J.-Z. Guo, H. Cui, S.-L. Xu, Y.-P. Dong, *J. Phys. Chem. C* **2006**, *110*, 606 – 611.

Received: May 27, 2014
Published online on September 9, 2014